Measuring the effect of post-weld heat treatment on residual stress relaxation in electron beam welds made of low alloy pressure vessel steel using the contour method

Ioannis D Pantelis, Mike C Smith, Anastasia N Vasileiou, Matthew J Roy

Measuring the effect of post-weld heat treatment on residual stress relaxation in electron beam welds made of low alloy pressure vessel steel using the contour method

Ioannis D. Pantelis[1,*], Mike C. Smith[1], Anastasia N. Vasileiou[1], Matthew J. Roy[1]

[1]*The University Of Manchester, Manchester, United Kingdom*

**Corresponding author:ioannis.pantelis@postgrad.manchester.ac.uk;*

ABSTRACT

Welding is of major importance for the nuclear industry as it affects safety, structural integrity and the life span of the nuclear power plant. The uneven thermal distribution and metallurgical misfits that develop during welding procedures introduce residual stresses, which can drive damage in safety-critical nuclear components. Post-weld heat treatment (PWHT) is known to reduce residual stresses, however, determining the PWHT parameters, such as hold temperature and soak time, needs to be standardized and not be based on judgement. Five 100mm thick electron beam welds were manufactured from SA508 Grade 3 Class 2 low alloy steel, four underwent four different PWHT schedules with differing hold temperatures and soak times, and one was retained in the as-welded (AW) state. The residual stresses in the as-welded condition were measured using incremental deep hole drilling and the contour method, while residual stresses after PWHT were measured using the contour method alone. All specimens exhibited the characteristic M-shaped stress distribution associated with solid-state phase transformation in the weld fusion zone and HAZ. The peak tensile stresses developed in untransformed parent material either side of the weld, and reached 650MPa in the as-welded state. Post-weld heat treatment resulted in significant relaxation, to between 100 and 200MPa.

Keywords: residual stress; post-weld heat treatment; contour method; SA508 steel; pressure vessel steel

1. Introduction

The Reactor Pressure Vessel (RPV) has both operational and safety functions, retaining the high pressure primary circuit fluid and forming one of the multiple barriers to fission product release in a light water reactor. A very low RPV failure probability is required during normal operation and postulated accident conditions (USNRC 1986, ASME 1986) [1]. The RPV should be made of materials that provide adequate levels of strength, ductility, fracture toughness and neutron-irradiation resistance [2]. Typically, the individual forged sections are made of low-alloy ferritic steels, such as ASME SA508, and these are joined using multi-pass arc welding techniques [3]. Electron beam welding has the potential to increase productivity (a single penetration pass to join large thick components), so is under active development for such applications [4][5][6][7].

Residual stresses arise as a consequence of the heterogeneous application of energy and uneven temperature distributions during welding [8][9] and have the potential to be a major contributor to in-service degradation of nuclear components [2][3]. In addition, welded ferritic structures undergo Solid State Phase Transformation (SSPT) in the weld fusion zone and adjacent heat-

affected zones during welding [12]. This has the potential both to alter the as-welded residual stress state and to introduce undesirable micro-constituents into weld and HAZ, adversely affecting the mechanical properties. Post-weld heat treatment (PWHT) is normally performed on low alloy pressure vessel steel components, both to reduce and redistribute residual stresses, and to restore the toughness of the weld region, by tempering any unwanted martensitic microstructures [13][14]. It is of vital importance to control the impact of PWHT parameters, like the holding temperature and time, in order to optimise both stress relaxation and mechanical properties. Electron beam welds differ from conventional arc welds in that they are both single-pass and autogenous, with no weld filler metal. It is not self-evident that post-weld heat treatment schedules developed for multi-pass arc welds are optimal for an EB weld. The present work addresses this issue, by comparing different residual stress measurement techniques used to estimate the residual stresses both after EB welding and after four different PWHT regimes.

2. Experimental procedures

The Nuclear Advanced Manufacturing Centre (NAMRC) manufactured five 100mm thick electron-beam welded butt welds made of SA508 Grade 3 Class 2 low alloy pressure vessel steel. The final components had dimensions 300mm x 300mm x 100mm.

2.1. Materials

The chemical composition and mechanical properties of SA508 Gr3 Cl2 steel are given in Table 1 and Table 2, respectively.

Table 1. Chemical composition of SA508 Gr3 Cl2 steel (wt.%)

C: 0.18	**Si**: 0.24	**Mn**: 1.32	**P**: 0.019	**S**: 0.022
Cr: 0.24	**Mo**: 0.53	**Ni**: 0.47	**Cu**: 0.052	**V**: 0.003
Nb: 0.004	**Ca**: 0.0004	**B**: 0.0001	**Ti**: 0.001	**Al**: 0.003

Table 2. Mechanical Properties of SA508 Gr3 Cl2 steel

Temperature (^{o}C)	**0.2% Proof Stress** (MPa)	**Tensile Strength** (MPa)	**Elongation** %	**Reduction of Area** %
Room Temp.	576	701	24	60

2.2. Weldment Manufacture and Non-Destructive Evaluation

The initial 300mm x 150mm x 100mm half coupons were electron beam welded using the NAMRC's K25 EBW facility. Initially, the half plates were tack-welded at the beam entry and exit points and a gutter bar was attached below the weld seam on the beam entry face. In order to diminish the probability of weld pool sagging, welding took place in the 2G position, and in order to prevent weld seam opening during welding, a sealing pass, at 10% beam current, took place, followed by a single penetration EBW pass. The penetration pass was produced by a 40kW gun, operated at 80kV, using an elliptical beam oscillation pattern with X and Y amplitudes of 2mm and 3mm, respectively and a 141Hz frequency. The temperature histories were measured using K-type thermocouples, spot-welded on the top and bottom surfaces. The welding parameters used are presented in Table 3.

Table 3. Electron Beam welding parameter set

	Beam Current (mA)	Lens Current (mA)	Travel Speed (mms^{-1})	Working Distance (mm)	Figure Pattern	Figure Amplitude X & Y (mm)	Figure Oscillation Frequency (Hz)
Sealing Pass	50	2185	5	295	0	0	0
Weld pass	500	1955	3.175	295	2	2 & 3	141

All welds underwent ultrasonic inspection and all were found to be free of volumetric defects. Slope-in and slope out defects were present at the beam entry and exit points, but these are of no significance for this study. Areas with lack of penetration defects were identified for two of the welds, but as these were located far from weld mid-length, they were also ignored. Acceptable areas of root concavity (less than 2mm deep) were also observed.

2.3. Post-weld Heat Treatment

With the aim of understanding, examining and optimising how residual stress relaxation occurs, four of the five specimens underwent four different post-weld heat treatments (PWHT), presented in Table 4.

Table 4. Experimental PWHT matrix for 100mm thick EB welds of SA508 Gr3 Cl2

	Temperature (+/- 10°C)	Hold time	Controlled cooling and heating rates above 290°C	Cooling below 290°C
A:	595°C	4 hr.	18°C/hr	Air cooling
B:	610°C	4 hr.	18°C/hr	Air cooling
C:	610°C	1 hr.	18°C/hr	Air cooling
D:	625°C	4 hr.	18°C/hr	Air cooling

2.4. Residual Stress Measurements

Residual stress measurements were made using the contour method (CM), deep hole drilling (DHD) and incremental deep hole drilling (iDHD), for the specimen in the as-welded condition, and using only the CM for the specimens in the PWHT condition. Two independent methods were applied to the as-welded plate to minimise uncertainties in the measured data, as advised by the R6 procedure [15], and to benchmark the performance of the contour method prior to its application to the heat treated plates.

The contour method is a destructive method for measuring and mapping residual stresses, proposed by Prime in 2001 [16] based on Bueckner's elastic superposition principle [17] and it involves the following steps:

- Rigidly clamping and cutting the specimen in half
- Estimating the resulting deformation by measuring the cut surfaces
- Processing the surface profile data (averaging, fitting and smoothing)
- Calculating the original residual stress distribution by conducting an FE analysis

The contour cuts were made in between pre-drilled 3mm pilot holes (ligaments), in order to minimize cutting-induced plasticity artefacts in the as-welded condition [18], and to simplify specimen clamping and support in the heat treated plates, using a wire electric discharge machine (EDM). The surfaces were measured by acquiring 7700 points per surface using a spacing between points equal to 1-1.2mm, using a Mitutoyo Crysta-Apex 776 coordinate measurement machine (CMM). The pre- and post- processing were conducted using Python Contour (pyCM), introduced by Roy et al [19]. The aligned and averaged surfaces were fitted to a bi-variate cubic spline with a knot spacing of 6mm in the transverse and normal direction, to reduce the noise, and the resulting 2D contour maps were produced using an FE mesh of quadratic elements, generated by 716 nodes spaced uniformly every 1.12mm along the perimeter of the surface, with a Young's Modulus E=191GPa and Poisson's Ratio ν=0.294. Displacement boundary conditions were set to prevent translation and rotation. Review of the measured stress fields suggested that the measurement spacing might have been insufficient to capture full details of the short wavelength M-shaped distribution expected in an EB-welded plate [20][21] , so to improve the measurements, one half-plate of the AW specimen was re-measured in the CMM machine with a higher point density corresponding to 204400 points and minimum distance between points equal to 0.23mm.

The deep hole drilling method is a semi-destructive, strain relief method, where strains are calculated during strain relief, produced by material removal [22]. A reference hole is gundrilled in-between reference bushes attached to the front and back surfaces. A cylinder of material containing the reference hole is cut, allowing for stress relaxation to occur, and the residual stresses are calculated by measuring the reference hole diameter prior and after the cut. To account for plasticity-induced errors, which will render the reference hole diameter measurements non-representative and thus, the measured residual stresses inaccurate, the incremental deep hole drilling method is employed, where the measurement of the reference hole diameter prior and after the EDM cut, occurs incrementally [23]. The DHD and iDHD measurements were performed transverse to the weld plane, for one of the AW half plates, at the facility of VEQTER LTD.

3. Results and discussion

3.1. Initial Residual Stress measurements using the contour method

Line plots on a transverse line at mid-thickness, were extracted and compared in Figure 1 for the AW and PWHT specimens using the initial full measurement data sets. We would expect to see a characteristic M-shape distribution, with peak tensile stresses just outside the HAZ and reduced stress levels within the HAZ and FZ, caused by the Solid State Phase Transformation during the EB welding procedure. There is some evidence of this in the heat-treated plates, but the as-welded plate appears to show a noticeable asymmetry, with peak stresses reaching 620MPa on the right side of the weld and only ~400MPa on the left side. It is tempting to attribute this to cutting induced plasticity effects, but it is also possible that the measurement point density or other aspects of the processing pipeline have created this effect. Outside the weld region, the residual stresses are small, with the exception of regions adjacent to the ligaments, where ''non-physical'' stress perturbations are observed due to measurement and fitting artefacts, produced by the pilot-holes. Removing the pilot holes from the analysis did not produce any significant improvement on the resulting data.

The effect of PWHT is also evident from the comparative plot with the RS dropping, for all four PWHT scenarios into the range of 100-200MPa. The characteristic M-shape distribution

and pilot-hole artefacts, were also observed, and small ‘’non-physical’’ tensile mean stresses, ranging from -50 to 100MPa, were present in the parent material. The reasons for this are not yet clear, although it should be remembered that the measured stresses outside the central weld region are close to the likely uncertainty in the technique.

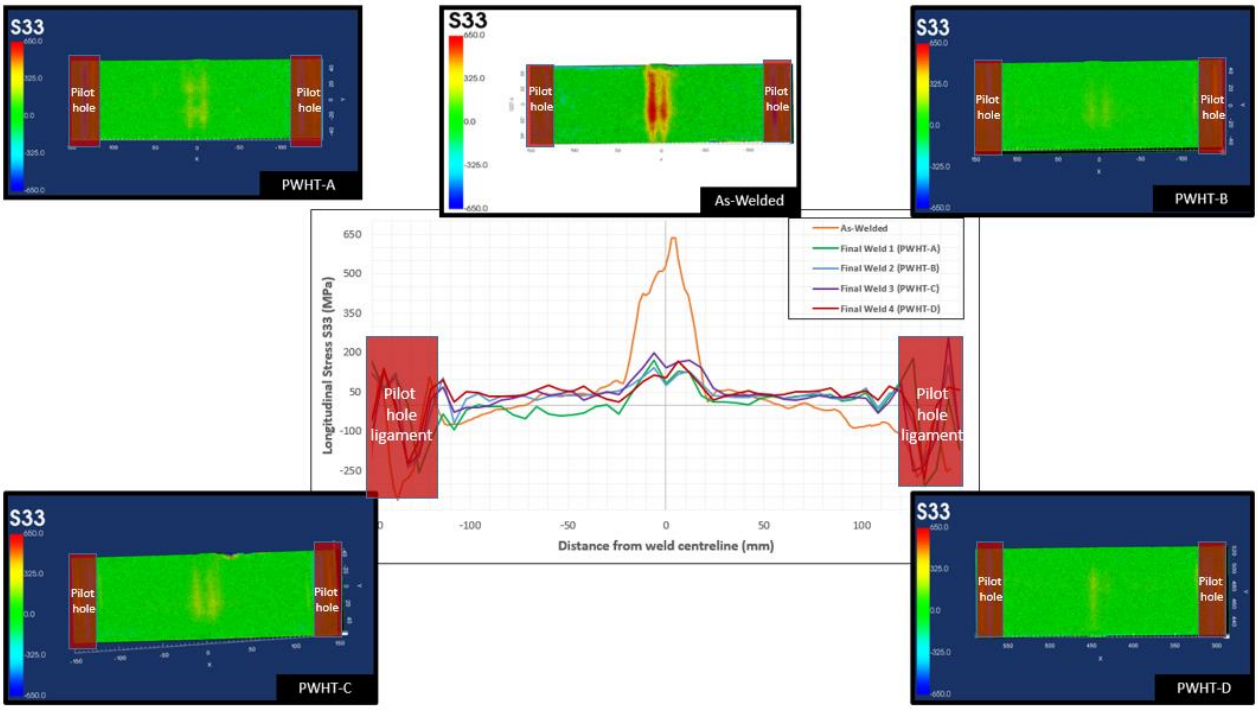

Figure 1. Comparative line plots of longitudinal component (S33) of residual stress in the EBW, in the AW and PWHT conditions, as measured by the contour method

3.2. Residual stress measurements using the DHD/iDHD method

Both DHD and iDHD measurements were performed on the AW specimen on a transverse line at weld mid-thickness, recovering both longitudinal and normal stresses, as seen on Figure 2. Both techniques revealed an M-shaped distribution in both components, with peak tensile stresses in parent material just outside the HAZ, a significant reduction in weld and HAZ caused by SSPT during welding, and a fall into compression further from the weld centerline. The iDHD measurements, as expected, recovered slightly higher peak tensile stresses, and both techniques showed some asymmetry in the peak stresses either side of the weld. These features are normally attributed to plasticity effects, which are less important in iDHD measurements, which thus show higher peak stresses and less asymmetry. Comparison with Figure 1 shows relatively poor agreement with the contour method measurement, so it is important to understand why this might be the case.

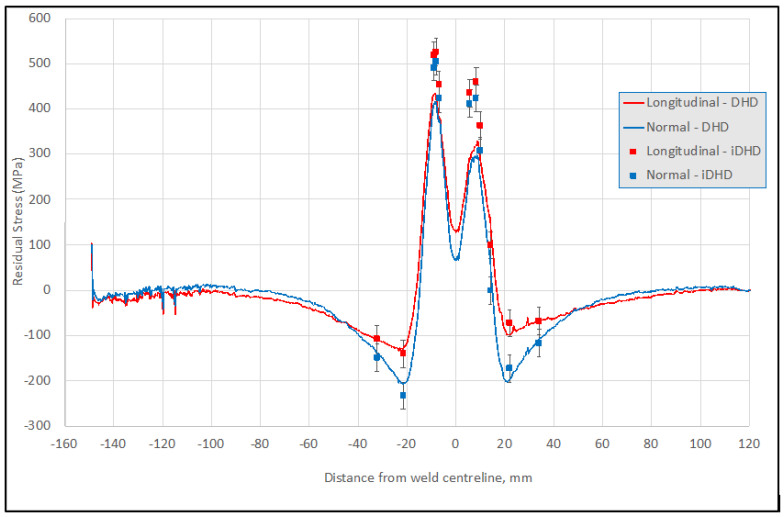

Figure 2. Incremental and conventional deep hole drilling measurements on AW plate on a transverse line at mid-thickness

3.3. Improvement of residual stress measurements using the contour method

For the purpose of improving the residual stress measurement of the AW specimen, and improve the accuracy of the method, only one half of the AW specimen was re-measured, without re-cutting, in the CMM machine with a higher point density, following the same pre-processing pipeline for the measured surface. A comparative plot, between the CM (coarse and refined point cloud) and DHD/iDHD methods, for the AW specimen, is presented in Figure 3.

It is observed that the refined point density, significantly changes the CM results. The asymmetry in the measured peak tensile stresses disappears, and the peak values are close to those measured using iDHD. Some disagreement remains, as the depression in stresses in weld and HAZ remains much less significant in the contour measurement, and it shows no evidence of a fall into compression outside the HAZ. Clearly the revised measurement is not perfect, as only one face of the cut was re-measured. However, it does show that the initial asymmetry was not due to cutting plasticity, but due to inadequate measurement point density. The density originally used would have been adequate for a multi-pass arc weld, which exhibits a longer wavelength residual stress distribution.

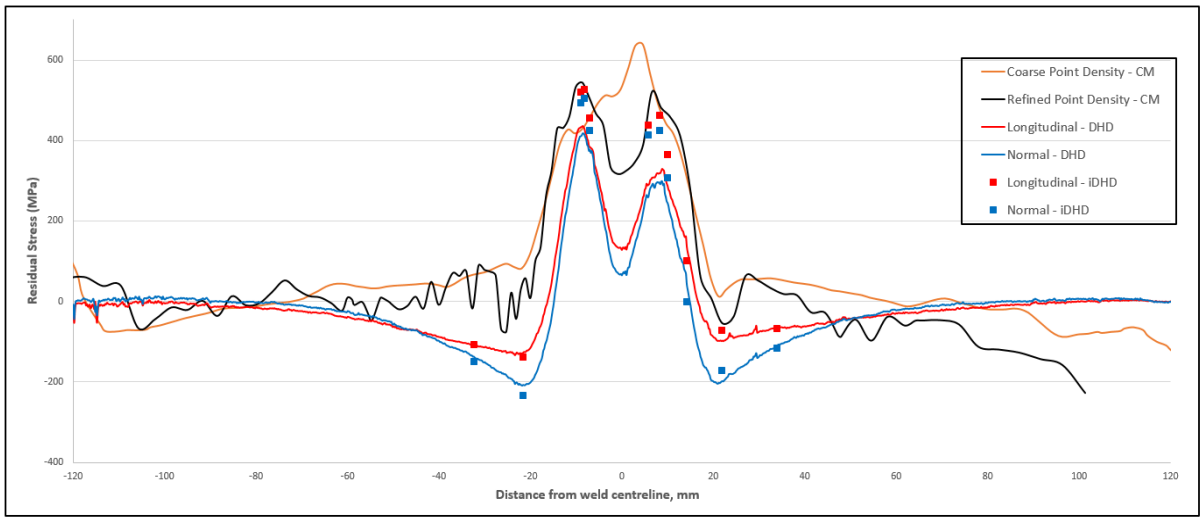

Figure 3. Comparative plot of longitudinal residual stress distribution on AW plate on a transverse line at mid-thickness, using the contour method (with coarse and fine point density), the deep hole drilling and the Incremental deep hole drilling method.

4. Conclusions

The following conclusions can be drawn from this study:

- The residual stress distribution, for all the welds (AW and PWHT) and all the methods (Contour Method, Deep Hole Drilling and incremental Deep Hole Drilling) followed the characteristic M-shape distribution, with tensile peak stresses present just outside the Heat Affected zone, that very rapidly fall down almost to zero in the far field.

- The contour method measurements are affected by the point density utilized during the cut-surface measurement step and a point density between 0.20mm and 0.25mm is found necessary to produce accurate results.

- The contour method, with the coarse point density, produced highly asymmetrical results, with tensile stresses of the order of ~450MPa in the FZ and peak tensile stresses of the order of ~620MPa just outside the HAZ. The peak tensile stresses, exceeded the offset 0.2% yield strength (576MPa).

- The contour method, with the fine point density, produced significantly less asymmetrical results and is in accordance with the incremental deep hole drilling measurements, with the residual stresses peaking at the range of 450-500MPa. The peak tensile stresses, did not exceed the offset 0.2% yield strength.

- The major difference between the CM, with the refined point density, and iDHD method, for the AW specimen, is the failure of the CM measurement to fall into compression outside the HAZ on each side.

- All four PWHT specimens present a significant residual stress relaxation, after heat treatment, with the stresses dropping in the range of 100-200MPa.

- After PWHT, significant pilot-hole artefacts were present, with the stresses at this region surpassing the measured stress in the FZ and HAZ. This is not realistic.

- After PWHT, the stresses in the parent material are ranging between -50MPa and +100MPa. This is also not realistic.

- It is not possible to rank the PWHT regimes based upon the current state of measurements. Measurements with a refined point density need to be conducted for the pilot-hole-related perturbations to be minimized in the data censoring and analysis

Acknowledgements

The authors are grateful to the NAMRC for producing the welded specimens and to VEQTER ltd for conducting the DHD and iDHD measurements. The authors would also like to thank Ian Winstanley and Paul English, at the University of Manchester, for technical assistance. Finally, the authors would like to acknowledge Rolls Royce Plc, for funding the PhD project, where this research was based on.

References

[1] G. R. Odette, “Nuclear Reactors: Pressure Vessel Steels,” in *Encyclopedia of Materials: Science and Technology*, 2001.

[2] P. P. Joshi, N. Kumar, and K. L. Murty, “Materials for Nuclear Reactors,” in *Encyclopedia of Materials: Metals and Allloys*, 2022.
[3] W. Guo, S. Dong, W. Guo, J. A. Francis, and L. Li, “Microstructure and mechanical characteristics of a laser welded joint in SA508 nuclear pressure vessel steel,” *Mater. Sci. Eng. A*, 2015, doi: 10.1016/j.msea.2014.11.056.
[4] B. Baufeld and T. Dutilleul, “Electron Beam Welding of Large Components for The Nuclear Industry,” *MATEC Web Conf.*, 2019, doi: 10.1051/matecconf/201926902009.
[5] G. R. Vadolia and K. Premjit Singh, “Electron Beam Welding: Study of process capability and limitations towards development of nuclear components,” 2017, doi: 10.1088/1742-6596/823/1/012040.
[6] A. Sanderson, “Four decades of electron beam development at TWI,” *Welding in the World*. 2007, doi: 10.1007/BF03266547.
[7] A. Sanderson, C. S. Punshon, and J. D. Russell, “Advanced welding processes for fusion reactor fabrication,” *Fusion Eng. Des.*, 2000, doi: 10.1016/S0920-3796(00)00407-5.
[8] P. J. Withers and H. K. D. H. Bhadeshia, “Residual stress part 1 - Measurement techniques,” *Materials Science and Technology*. 2001, doi: 10.1179/026708301101509980.
[9] J. A. Francis, H. K. D. H. Bhadeshia, and P. J. Withers, “Welding residual stresses in ferritic power plant steels,” *Materials Science and Technology*. 2007, doi: 10.1179/174328407X213116.
[10] A. J. Allen, R. Coppola, M. T. Hutchings, M. Valli, and C. G. Windsor, “Study of residual stress in a ferritic steel electron beam test weldment using neutron diffraction,” *Mater. Lett.*, 1995, doi: 10.1016/0167-577X(95)00028-3.
[11] S. Maddox, “Influence of Tensile Residual Stresses on the Fatigue Behavior of Welded Joints in Steel,” in *Residual Stress Effects in Fatigue*, 2009.
[12] A. N. Vasileiou, M. C. Smith, J. Balakrishnan, J. A. Francis, and C. J. Hamelin, “The impact of transformation plasticity on the electron beam welding of thick-section ferritic steel components,” *Nucl. Eng. Des.*, 2017, doi: 10.1016/j.nucengdes.2017.03.040.
[13] K. R. Ayres *et al.*, “Development of reduced pressure electron beam welding process for thick section pressure vessel welds,” 2010, doi: 10.1115/PVP2010-25957.
[14] D. W. Rathod *et al.*, “Residual stresses in arc and electron-beam welds in 130 mm thick SA508 steel: Part 1 - Manufacture,” *Int. J. Press. Vessel. Pip.*, 2019, doi: 10.1016/j.ijpvp.2019.03.034.
[15] EDF Energy, *R6, Assessment of the integrity of structures containing defects*. 2015.
[16] M. B. Prime, “Cross-Sectional Mapping of Residual Stresses by Measuring the Surface Contour After a Cut,” *J. Eng. Mater. Technol.*, vol. 123, no. 2, p. 162, 2001, doi: 10.1115/1.1345526.
[17] H. Bueckner, “The propagation of cracks and the energy of elastic deformation,” *Trans. Am. Soc. Mech. Eng.*, pp. 1225–1230, 1958.
[18] Y. Traore, P. J. Bouchard, J. Francis, and F. Hosseinzadeh, “A novel cutting strategy for reducing plasticity induced errors in residual stress measurements made with the contour method,” 2011, doi: 10.1115/PVP2011-57509.
[19] M. J. Roy, N. Stoyanov, R. J. Moat, and P. J. Withers, “pyCM: An open-source computational framework for residual stress analysis employing the Contour Method,” *SoftwareX*, 2020, doi: 10.1016/j.softx.2020.100458.
[20] A. N. Vasileiou, M. C. Smith, D. Gandy, A. Ferhati, R. Romac, and S. Paddea, “Residual stresses in thick-section electron beam welds in RPV steels,” 2016, doi: 10.1115/PVP2016-63940.
[21] A. N. Vasileiou *et al.*, “Development of microstructure and residual stress in electron beam welds in low alloy pressure vessel steels,” *Mater. Des.*, 2021, doi: 10.1016/j.matdes.2021.109924.
[22] D. J. Smith, “Deep Hole Drilling,” in *Practical Residual Stress Measurement Methods*, .
[23] A. H. Mahmoudi, S. Hossain, C. E. Truman, D. J. Smith, and M. J. Pavier, “A new procedure to measure near yield residual stresses using the deep hole drilling technique,” *Exp. Mech.*, 2009, doi: 10.1007/s11340-008-9164-y.